Prolonged release of bone morphogenetic protein-2 in vivo by gene transfection with DNA-functionalized calcium phosphate nanoparticle-loaded collagen scaffolds

doi: 10.1016/j.msec.2018.06.047

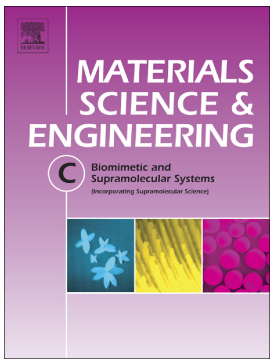

Prolonged release of bone morphogenetic protein-2 in vivo by gene transfection with DNA-functionalized calcium phosphate nanoparticle-loaded collagen scaffolds

Taichi Tenkumo, Juan Ramón Vanegas Sáenz, Keisuke Nakamura, Yoshinaka Shimuzu, Viktoriya Sokolova, Matthias Epple, Yuya Kamano, Hiroshi Egusa, Tsutomu Sugaya, Keiichi Sasaki

PII: S0928-4931(17)31451-0
DOI: doi:10.1016/j.msec.2018.06.047
Reference: MSC 8686

To appear in: *Materials Science & Engineering C*

Received date: 20 April 2017
Revised date: 13 June 2018
Accepted date: 21 June 2018

Please cite this article as: Taichi Tenkumo, Juan Ramón Vanegas Sáenz, Keisuke Nakamura, Yoshinaka Shimuzu, Viktoriya Sokolova, Matthias Epple, Yuya Kamano, Hiroshi Egusa, Tsutomu Sugaya, Keiichi Sasaki , Prolonged release of bone morphogenetic protein-2 in vivo by gene transfection with DNA-functionalized calcium phosphate nanoparticle-loaded collagen scaffolds. Msc (2018), doi:10.1016/j.msec.2018.06.047

Prolonged Release of Bone Morphogenetic Protein-2 *In Vivo* by Gene Transfection with DNA-Functionalized Calcium Phosphate Nanoparticle-Loaded Collagen Scaffolds

Taichi Tenkumo,[a*] Juan Ramón Vanegas Sáenz,[b] Keisuke Nakamura,[a] Yoshinaka Shimuzu,[c] Viktoriya Sokolova,[d] Matthias Epple,[d] Yuya Kamano,[e] Hiroshi Egusa,[e] Tsutomu Sugaya,[f] Keiichi Sasaki.[b]

[a] *Laboratory for Redox Regulation, Tohoku University Graduate School of Dentistry, 4-1 Seiryo-machi, Aoba-ku, Sendai, 980-8575, Japan*

[b] *Division of Advanced Prosthetic Dentistry, Tohoku University Graduate school of Dentistry, 4-1 Seiryo-machi, Aoba-ku, Sendai, 980-8575, Japan*

[c] *Division of Oral Pathology, Tohoku University Graduate School of Dentistry, 4-1 Seiryo-machi, Aoba-ku, Sendai, 980-8575, Japan*

[d] *Institute for Inorganic Chemistry and Center for Nanointegration Duisburg-Essen (CeNIDE), University of Duisburg-Essen, Universitaetsstr. 5-7, 45117 Essen, Germany*

[e] *Division of Molecular and Regenerative Prosthodontics, Tohoku University Graduate School of Dentistry, 4-1 Seiryo-machi, Aoba-ku, Sendai, 980-8575, Japan*

[f] *Department of Periodontology and Endodontology, Division of Oral Health Science, Graduate School of Dental Medicine, Hokkaido University, W7 Kita-ku, Sapporo 060-8586, Japan*

*Correspondence to:

Taichi Tenkumo.

Laboratory for Redox Regulation

Tohoku University Graduate School of Dentistry

4-1 Seiryo machi, Aoba-ku, Sendai

980-8575, JAPAN

Email: ta.tenkumo@gmail.com

Abstract

In the combination of scaffolds immersed in growth factor solutions, the release of growth factors mainly depends on scaffold degradation. However, the release of bone morphogenetic protein (BMP)-2 at an appropriate concentration during the stage of tissue regeneration would enhance bone regeneration. To achieve this condition, the present study was performed to investigate the effects of scaffolds combined with gene transfection using non-viral vectors. Nanohydroxyapatite-collagen (nHAC) scaffolds cross-linked with 1-ethyl-3-(3-dimethylaminopropyl) carbodiimide hydrochloride (EDC) or ascorbic acid/copper chloride, and a collagen scaffold (Terdermis®) were prepared, loaded with BMP-2-encoding plasmid DNA-functionalized calcium phosphate nanoparticles (CaP), naked plasmid DNA, or BMP-2 solution, and implanted in rats. The yield of released BMP-2 and its releasing period, respectively, were larger and longer from the scaffolds loaded with CaP than from those incubated with BMP-2 solution. In addition, the alkaline phosphatase activity induced by the CaP-loaded scaffolds was higher. Histological analysis showed that released BMP-2 could be observed on the macrophages or multinuclear giant cells surrounding the nHAC fragments or collagen fibres. TRAP-positive or OCN-positive sites were observed in all groups and a mineralization area was observed in the Terdermis®/CaP sample. The present study demonstrates that gene transfection by scaffold loaded with CaP gene transfer vectors induces a larger yield of BMP-2 for a longer period than by scaffolds loaded with BMP-2 solution or naked plasmid.

Keywords: Calcium Phosphate, Nanoparticle, Biomedical Application, Tissue Engineering, Drug Delivery

1 Introduction

Cells, signalling molecules such as growth factors, and scaffolds comprise the basic elements necessary for tissue engineering [1]. Previously, numerous scaffolds loaded with different growth factors have been developed and applied *in vivo* for the effective regeneration of tissue, such as bone [2–5] and periodontal tissue [6–9]. For these applications, it was demonstrated that the combination of calcium phosphate-based scaffolds and bone morphogenetic protein (BMP)-2, a bone growth factor, enhanced the regeneration of bone and cementum in periodontal tissue [9]. During bone healing, several fundamental processes such as inflammation and angiogenesis occur at an early stage, followed by a tissue regeneration stage in which growth factors play an important role in tissue reconstruction [10]. In many studies, the combination of scaffold and growth factors has been fabricated by immersing the scaffold into a growth factor-containing solution [3–9]. In this method, the release of the growth factor from scaffolds is dependent on scaffold degradation; furthermore, activity of the growth factor rapidly declines in a time-dependent manner [11–13]. Thus, it is difficult to release an adequate quantity of the growth factors during the stage of tissue regeneration. To obtain sufficient growth factor yield during bone regeneration, a high dose of BMP-2 is loaded on the scaffolds. However, the release of BMP-2 at a high level over a short period adversely induces bone or tooth resorption [5,14,15]. Therefore, the release of BMP-2 at an appropriate concentration during the stage of tissue regeneration is considered a favourable condition to induce bone regeneration.

To achieve the gradual release of growth factors, we have focused on gene transfection techniques. The application of scaffolds loaded with viral vectors has been successfully demonstrated by both *in vitro* and *in vivo* studies [16,17]. In addition, owing to the risk of mutation and associated pathogenicity of viral vectors [18], numerous non-viral vectors, such as cationic polymers [19–21], cationic peptides [22–24], and inorganic nanoparticles [25–31] that carry a lower risk than viral vectors [18] have been developed. Among these vectors,

calcium phosphate-based gene transfer is attractive because of its high biocompatibility. Calcium phosphate represents the main component of hard tissues including bones and teeth and exhibits high compatibility with various peptides, DNA, siRNA, and proteins [27]. In particular, we have previously developed a technique to effectively induce gene transfection using multi-shell calcium phosphate nanoparticles loaded with peptides [29]. In addition, a recent *in vitro* study demonstrated that the gene transfection of human mesenchymal stem cells by a nanohydroxyapatite-collagen (nHAC) scaffold loaded with DNA-functionalized calcium phosphate nanoparticles (CaP) encoding BMP-2 resulted in growth factor release over 10 days [30]. However, the response of cells *in vivo* is more complex than that of cells *in vitro* conditions. Furthermore, few *in vivo* studies have analysed the yield of growth factor consequent to non-viral gene transfection using DNA-functionalized scaffolds.

Accordingly, the object of the present study was to investigate the yield, releasing period, and activity of BMP-2 produced *in vivo* by gene transfection using biodegradable scaffolds, and to compare the influence of scaffold type on BMP-2 release.

2 **Materials and methods**

2.1 Design of a Growth Factor Releasing System from Scaffolds

Figure 1 shows the schematic concept of the growth factor releasing system from nHAC loaded with DNA-functionalized CaPs. When implanted *in vivo*, the scaffold is degraded with time. The gene transfer vectors are gradually released depending on the degradation rate of the scaffold and cells invading around or into the scaffold take up the vector. Then, the vector enters the nucleus of the cell, causing the cell to eventually release BMP-2. Thus, the sustained release of BMP-2 is achieved depending on the gene transfection efficiency.

2.2 Preparation of Scaffolds Loaded with Functionalized Nanoparticles

The fabrication procedure of the nHAC scaffold loaded with DNA-functionalized nanoparticles was described in our previous study [30]. Briefly, for fabrication of nHAC scaffolds, HCl (0.01 M) solution with purified type I atelocollagen gel (1 mg·mL^{-1}; 2 wt%, Koken Co., Japan) was mixed with KH_2PO_4/K_2HPO_4 and Tris-buffer (0.5 M, pH 7.4). Subsequently, $CaCl_2$ solution (0.1 M) was added to the mixture at 4 °C to effect the mineralization of collagen fibrils. After incubation for 12 h at 37 °C, white precipitate of mineralized collagen was collected by centrifugation. The pellet was resuspended in distilled water and transferred to a 96-well plate to obtain a cylindrical shape (diameter: 6.4 mm) by centrifugation at 698.75 *g*. Then, the formed scaffolds were cross-linked by 1-ethyl-3-(3-dimethylaminopropyl) carbodiimide hydrochloride (EDC) (Kanto Chemical, Japan) (1 wt%) in ethanol (80 vol%) or ascorbic acid (80 vol%)/copper chloride (0.05 mM) solution (AA/CC) for 1 h. The prepared scaffolds were quenched with 1% glycine and rinsed with distilled water several times to remove any remaining activated carbodiimide hydrochloride. Subsequently, nHAC was processed by freeze-drying for 12 h (0.08 mbar, −80 °C), resulting in shrinkage by approximately 0.3 mm in diameter, irrespective of cross-linking agents. After freeze-drying, the nHAC was sliced to be 2 mm thick. Thus, the volume of the scaffolds was 60.4 mm^3 (3.1 mm × 3.1 mm × 3.14 × 2 mm). The prepared nHAC scaffolds were classified according to cross-linking agent and termed as EDC-nHAC and AACC-nHAC, respectively. The collagen scaffold, Terdermis® (Olympus Terumo Biomaterials Co, Japan), was also tested. To obtain the same volume, Terdermis® was cut to the size of 5.5 mm × 5.5 mm × 2 mm (60.5 mm^3).

For the preparation of DNA-functionalized CaP nanoparticles, aqueous solutions of pUC57-BMP-2 (GenScript, USA) (1 mg·mL^{-1}; 9.6 µL) and protamine (Wako, Japan) (10 mg·mL^{-1}; 4.8 µL) were mixed. Plasmid DNA was purified from *Escherichia coli* using the Plasmid Giga kit (QIAGEN, Germany). Plasmid DNA and protamine complex were added to an aqueous CaP nanoparticle dispersion (36 µL), which was prepared by mixing equal volumes of an aqueous solution of calcium nitrate (18 mM, pH 9.0) and diammonium

hydrogen phosphate solution (10.8 mM, p H 9.0) using a peristaltic pump. Subsequently, calcium nitrate (18 µL) and diammonium hydrogen phosphate (18 µL) solutions were added into the prepared dispersion and mixed, followed by the addition of an aqueous solution of protamine sulphate (10 mg·mL^{-1}; 9.6 µL). The obtained CaP nanoparticle suspension was purified at 193,548 *g* for 30 min in order to remove excess polymer and peptide. After removal of the supernatant, the CaP nanoparticles were redispersed in fresh distilled water for 10 s using an ultrasonicator (UR-20P, Tomy, Japan; frequency: 21 kHz). Figure 1b shows the schematic image of the CaP nanoparticle gene vector. The multi-shell structure of the CaP nanoparticles was demonstrated in our previous reports [25, 29, 30].

nHACs loaded with DNA-functionalized CaP (nHAC/CaP) were generated by the injection of CaP nanoparticle dispersions into the nHAC with a volume of 60.4 mm^3. The prepared nHAC/CaP was classified by the concentration of CaP nanoparticles as follows: nHAC only, nHAC/CaP 2, nHAC/CaP 4, nHAC/CaP 10, nHAC/CaP 20, and nHAC/CaP 40, respectively.

As control samples, for nHAC scaffold loading with naked plasmid DNA without CaP, nHAC was injected with 9.8 µL plasmid DNA encoding BMP-2 (1 mg·mL^{-1}) (nHAC/Plasmid); for nHAC scaffold including BMP-2 solution, nHAC was immersed in BMP-2 solution (Promokine, Heidelberg, Germany) (3 ng·mL^{-1}) for 10 min prior to implantation according to our previous report (nHAC/solution) [5]. Finally, the prepared scaffolds were subjected to a re-freeze-drying process for 12 h (0.08 mbar, −80 °C) and stored at −80 °C for 3 weeks until implantation. Terdermis® loaded with CaP was fabricated by immersing the formed Terdermis® into the various concentrations of CaP nanoparticle dispersions and classified as follows: Terdermis® only, Terdermis®/CaP 2, Terdermis®/CaP 4, Terdermis®/CaP 10, Terdermis®/CaP 20, and Terdermis®/CaP 40, respectively. Additionally, for Terdermis® loading with naked plasmid DNA without CaP, formed Terdermis® was also injected with 9.8 µL plasmid DNA encoding BMP-2 (1 mg·mL^{-1}) (Terdermis®/Plasmid); for

Terdermis® including BMP-2 solution, formed Terdermis® was immersed into BMP-2 solution (3 ng·mL^{-1}) for 10 min (Terdermis®/solution). The components of the prepared scaffolds are shown in Table 1. Characterization of the fabricated scaffolds was performed using scanning electron microscopy (JSM-7800F, JEOL, Japan) following carbon-palladium alloy sputtering.

2.3 Surgical Procedures

All animal experimental protocols were reviewed and approved by the Institutional Animal Experiment Committee of Tohoku University (Approval number: 2015shidou-046) prior to beginning the animal experiments. In total, 96 male Wistar rats (8 weeks old) were used for this experiment in accordance with the guide for the care and use of laboratory animals of Tohoku University. The rats were anesthetized with an intraperitoneal injection of medetomidine (Domitor®, 0.375 mg·kg^{-1} body weight; Nippon Zenyaku Kogyo, Japan), midazolam (Sandoz®, 2 mg·kg^{-1} body weight; Sandoz, Japan), and butorphanol tartrate (Vetorphale®, 2.5 mg·kg^{-1} body weight; Meiji Seika Co., Japan). The prepared scaffolds were implanted into subcutaneous tissue of the back of the rats. After implantation, the flap was rigidly sutured to prevent infection and loss of the scaffolds. The rats were sacrificed using an overdose of sodium pentobarbital (Somnopentyl®, Kyoritsu Seiyaku Co., Japan) at 4, 7, 14, 21, or 28 days after surgery, and the tissue surrounding the implants was extracted. Each extracted tissue was subjected to different procedures for the following analyses.

2.4 Degradation Magnitude and New Mineralization of the nHAC Scaffold

The extracted tissue was immediately fixed in formalin solution (10%) for micro-computed tomography and histological processing. To determine the magnitude of nHAC degradation and newly formed mineralization, the extracted tissue including nHAC was scanned by micro-computed tomography (ScanXmate-E090, Camscan Techno Co, Japan) (60 kV; 80 μA). The

volumes of the samples were measured using 3D structural analysis software (TRI/3D-VEI, Patoc System Engineering. Co. Ltd., Japan). The volumes of non-implanted EDC- or AA/CC-nHACs were regarded as controls. The degradation magnitude was calculated as the percentage of the sample against non-implanted scaffold. For measurement of the newly formed mineralization volume or the remaining scaffold volume, the tissue volume of the specimens was calculated. The mean value of these samples was established as a measured value. The volume of the remaining Terdermis® scaffolds could not be measured by micro-computed tomography owing to the low X-ray mass absorption coefficient of collagen. Thus, the degradation of Terdermis® was only observed in the histological sections.

2.5 Histological Evaluation

After micro-CT analysis, the extracted tissue was decalcified in 17.7% EDTA (OSTEOSOFT®, Merck Millipore, Japan) and then embedded in paraffin. The tissue sections (5-μm thick) were stained with haematoxylin and eosin (H-E) and Masson Trichrome. Tartrate-resistant acid phosphatase (TRAP) activity or osteocalcin (OCN) activity was identified using a TRAP/ALP stain kit (WAKO, Japan) or Anti-Rat Osteocalcin, Monoclonal antibody (Clone 6-7H)® (TaKaRa Bio, Japan, 1:2000 dilution in phosphate buffered saline (PBS)) in accordance with the respective manufacturer instruction.

For identification of type 1 or type 2 macrophages, the tissue sections were stained with Anti CD86 (Proteintech, Japan, 1:500 dilution in PBS) or Anti CD206 (Proteintech, 1:500 dilution in PBS) antibody, respectively. For the evaluation of BMP-2 release, the decalcified sections were immunohistochemically stained with an anti-BMP-2 antibody (Anti-BMP-2, Rabbit-Poly (anti-Bone Morphogenic Protein2) ®, Novus Biological, USA, 1:250 dilution in PBS). Briefly, tissue sections were incubated with the anti-BMP-2 antibody at 4 °C overnight. After an extensive wash with PBS solution, bound antibodies were detected with the Histofin® Simple Stain MAX PO (R) reagent (Nichirei Biosciences, Tokyo, Japan), using

diaminobenzidine tetrahydrochloride as the substrate. For measurement of the newly formed mineralization area and the remaining scaffold area, three H-E-stained sections were taken from scaffold/Cap 40 after implantation; one approximately from the centre of the scaffold, and the other two at 100 μm from either side of the centre. The mean value of these three sections was established as a measured value. For calculation of the ratio of BMP-2 staining cells/ total cells, three areas (200 μm × 200 μm) were selected from the BMP-2-stained sections. Histological measurements were obtained using Image J (National Institutes of Health). The prepared sections were observed under a light microscope.

2.6 Biochemical Evaluation

To determine the yield of released BMP-2, the extracted tissue (250 mg) was freeze-dried and crushed according to a method reported by Yamamoto *et al* [12]. The crushed tissue was dissolved in RIPA Lysis Buffer® solution (Santa Cruz Biotechnology, Inc., USA) (600 μL) and homogenized by ultrasonic treatment for 10 s, followed by centrifugation at 16,099 *g* for 15 min. The supernatant was subjected to enzyme-linked immunosorbent assay (ELISA) for quantification of BMP-2 using the Human BMP-2 ELISA Development Kit® (Promokine). The absorbance of the reaction mixture at 450 nm and 650 nm was measured according to manufacturer instruction using a microplate reader (Spectra MAX 190, Molecular Devices, Japan).

For the determination of alkaline phosphatase (ALP), or OCN activity, the homogenized solution was also prepared as described above. After centrifugation, the supernatant was analysed using LabAssay ALP (Wako) or the Osteocalcin EIA kit (Funakoshi, Tokyo, Japan) in accordance with the respective manufacturer protocol.

2.7 Statistical Analysis

All the values in biochemical measurements are shown as the means ± standard deviation. Statistical analyses were performed using JMP Pro 13.1.0 software (SAS Institute, Cary NC, USA). A linear mixed model was used to infer the BMP-2 concentration, as well as ALP and OCN activity. Sample type, observation time, and their interaction term were set as explanatory variables. Statistical differences between each group were assessed using the Tukey-Kramer HSD multiple comparison test.

3 Results

3.1. SEM observation of prepared scaffolds

Figure 2 shows scanning electron microscopy images of the scaffolds. The EDC- and AA/CC-nHAC scaffolds exhibited porosity with a pore size of 50–500 μm (Figure 2a, b). Both EDC- and AA/CC-nHAC scaffolds showed a rough surface composed of needle shape-like crystals (Figure 2d, e), which we previously demonstrated were composed of hydroxyapatite [5]. Terdermis® also exhibited porosity with a pore size of 100–500 μm (Figure 2c), although the surface was relatively flat without crystals (Figure 2f). When loaded with CaP, spherical shape-like nanoparticles with a diameter of 200–400 nm were observed as being scattered over all the surface on both nHAC and Terdermis® scaffolds (Figure 2g-i).

3.2. In vivo release of BMP-2 from scaffolds

Figure 3 shows the yield of BMP-2 in the tissue surrounding the scaffold. In the EDC-nHACs loaded with DNA-functionalized CaP (EDC-nHAC/CaP) group, for nHAC/CaP 40 samples, the released BMP-2 yield was 5.4 ± 0.6 ng·mL^{-1} at 4 days and constantly over 5.0 ng·mL^{-1} at any time point, whereas for the other nHAC/CaP groups, the released BMP-2 yield increased in a time dependent manner (Figure 3a). The BMP-2 yield of nHAC only (without CaP) was lower than that of nHAC/CaP at any time point. Although the BMP-2 concentration of nHACs incubated in BMP-2 solution (EDC-nHAC/solution) or nHAC

loaded with naked plasmid DNA (EDC-nHAC/Plasmid) was as high as 3.0 ± 0.7 , 3.1 ± 0.2 ng·mL^{-1} at 7 days, respectively, it subsequently decreased, becoming significantly lower than that of nHAC/CaP after 21 days. In the AA/CC-nHAC/CaP group, for nHAC/CaP 40 samples, the released BMP-2 yield was 6.2 ± 0.8 ng·mL^{-1} at 4 days and also constantly over 5.0 ng·mL^{-1} at any time point, whereas for the other nHAC/ CaP groups, the concentration of BMP-2 increased with time, as was seen for EDC-nHAC/CaP (Figure 3b). For nHAC/solution or nHAC/plasmid, the peak of BMP-2 concentration was 2.5 ± 1.5 or 3.6 ± 1.5 ng·mL^{-1} at 7 days, respectively, which then decreased. The BMP-2 concentration in nHAC/CaP was significantly higher than that of nHAC/solution after 21 days. In the Terdermis® group, only the BMP-2 concentration of Terdermis®/CaP 40 was over 4.5 ng·mL^{-1} at any time point and was significantly higher than that of the other Terdermis® /CaP groups from 21 days (Figure 3c). The BMP-2 concentration of the other Terdermis®/CaP and Terdermis®/solution groups decreased in a time-dependent manner, although those of the Terdermis®/CaP groups were significantly higher than that of the Terdermis® only sample until 14 days. For Terdermis®/plasmid, the BMP-2 concentration was not significantly different from that of the Terdermis® only sample at any time point.

Figure 3d shows the comparison of the released BMP-2 concentration from different scaffolds combined with CaP 40. The peak of BMP-2 concentrations of EDC-or AA/CC-nHAC/CaP 40 were 7.7 ± 0.6 ng·mL^{-1} at 21 days or 7.1 ± 1.7 ng·mL^{-1} at 14 days, respectively, which were significantly higher than that of Terdermis®/CaP 40 (4.6 ± 1.4 ng·mL^{-1} and 5.2 ± 1.7 ng·mL^{-1} at 21 and 14 days, respectively). In contrast, the peak of BMP-2 concentration of Terdermis®/CaP 40 was 6.1 ± 1.4 ng·mL^{-1} at 7 days, although this was not significantly different from that of either EDC- or AA/CC-nHAC/CaP 40 (5.8 ± 0.3 or 5.5 ± 0.2 ng·mL^{-1}, respectively) at 7 days.

Figure 4a shows the degradation ratio of both nHAC scaffolds without CaP nanoparticles implanted in rat subcutaneous tissue. The degradation of both nHAC scaffolds was dependent

on the time after implantation. EDC-nHAC was degraded to half of its original volume by 7 days and only 9% remained at 28 days. Analogously, the AA/CC-nHAC was degraded to half volume by 7 days and only 13% remained at 28 days. Figure 4b and 4c show the relationship of the BMP-2 concentration released from nHAC/CaP 40, nHAC/CaP 10, or nHAC/solution to the remaining percentage of EDC-nHAC and AA/CC-nHAC scaffolds, respectively. The coefficient of determination (R^2) in EDC-nHAC/CaP 10 and AA/CC-nHAC/CaP 10 samples was 0.87 and 0.92, respectively. The slopes of both nHAC/CaP 10 samples were −0.1 and showed that the yield of released BMP-2 was in inverse proportion to the degradation of nHAC scaffolds, whereas those of EDC-nHAC/solution and AA/CC-nHAC/solution samples were 0.04 and 0.03 and showed direct proportions. The coefficient of determination (R^2) in EDC-nHAC/CaP 40 and AA/CC-nHAC/CaP 40 samples was 0.25 and 0.17, respectively, representing low values. The slope of the EDC- or AA/CC-nHAC/CaP 40 sample was −0.02 or 0.02 and indicated constant release independent of the degradation of the nHAC scaffold.

For the Terdermis® only scaffold, numerous collagen fibres could be seen at 28 days following histological examination, which indicated that the collagen fibres of the Terdermis® scaffold were retained at every point in this study (data not shown).

3.3. ALP and OCN activity

Figure 5 shows ALP activity in the tissue surrounding the scaffold. ALP activity for EDC-nHAC/CaP increased over time (Figure 5a). EDC-nHAC/solution or EDC-nHAC/plasmid showed ALP activity of approximately 0.2–0.5 nmol·mL^{-1} at any time point, which was significantly lower than that of nHAC/CaP after 14 days. In the AA/CC-nHAC/CaP, ALP activity increased with time, as was seen for EDC-nHAC/CaP (Figure 5b). The ALP activity of nHAC only was substantially lower than that of nHAC/CaP. For AA/CC-nHAC/solution or AA/CC-nHAC/plasmid, the ALP activity was approximately 0.3 or 0.5 nmol·mL^{-1} at 7 and

14 days, respectively, and then decreased. For the Terdermis®/CaP scaffolds, in only the CaP 40 sample, ALP activity increased up to 28 days, whereas in the other CaP groups, ALP activity increased up to 14 days and then decreased (Figure 5c).

Figure 6 shows OCN activity in the tissue surrounding the scaffold at 28 days after implantation of EDC-nHAC/CaP 40, AA/CC-nHAC/CaP 40, and Terdermis®/CaP 40. The OCN concentration of EDC-nHAC/CaP 40, AA/CC-nHAC/CaP 40, and Terdermis®/CaP 40 was 1.2 ± 0.2, 1.5 ± 0.2, and 1.4 ± 0.3 ng·mL^{-1}, respectively, which was significantly higher than that of subcutaneous tissue only sample (0.2 ± 0.05 ng·mL^{-1}).

3.4. Histological observation of implanted scaffolds incorporating CaP

Figure 7 shows the immunohistochemical analysis of the back subcutaneous tissue at 4 and 28 days after implantation of EDC-nHAC/CaP 40, AA/CC-nHAC/CaP 40, and Terdermis®/CaP 40. In either EDC- or AA/CC-nHAC/CaP, the nHAC scaffold was degraded into small pieces and mononuclear cells or multinuclear giant cells were observed around or inside of the graded nHAC pieces at 4 days (Figure 7a, b), some of which were strongly positive for BMP-2 staining (Figure 7d, e). The nHAC scaffold at 28 days was degraded into smaller pieces than that of 4 days (Figure 7g, h, j, k). For Terdermis®, surrounding mononuclear cells or intra-collagen fibres were stained as BMP-2-positive at 4 days (Figure 7f), whereas fibroblast-like cells surrounding collagen and collagen fibres were stained at 28 days (Figure 7l). For EDC- or AA/CC-nHAC/CaP 10, surrounding mononuclear cells or intra-collagen fibres were stained as BMP-2-positive, respectively, as was seen for EDC-or AA/CC-nHAC/CaP 40 (Figure 7p, q). For Terdermis®, few fibroblasts and collagen fibres in the implanted area were stained (Figure 7r).

Figure 8 and 9 show the histological findings of the back subcutaneous tissue at 28 days after implantation of EDC-nHAC/CaP 40, AA/CC-nHAC/CaP 40, and Terdermis®/CaP 40. No severe inflammation, necrosis, or drainage was observed in any group. nHAC scaffolds

were degraded into small size and the cells infiltrated into the inside or intra-degraded nHAC pieces in EDC-or AA/CC-nHAC/CaP 40 samples (Figure 8a,b, c, d, g, h). In either EDC-or AA/CC-nHAC/CaP 40 samples, ectopic bone formation could not be clearly observed (Figure 8a, b, d, e), as mononuclear cells or multinuclear giant cells stained with TRAP (Figure 9a, b) and OCN (Figure 9d, e) were observed around or inside of nHAC. CD206- as well as CD86-positive cells were observed around the degraded nHAC fragments in both EDC- and AA/CC-nHAC/CaP40 samples (Figure 8j, k, m, n). Finally, for Terdermis®/CaP 40, the retained collagen fibres were observed and fibroblast-like cells were observed (Figure 8c, f, i). The mineralization area was observed around the location where the mononuclear and multi-nuclear giant cells stained by TRAP (Figure 9c) or OCN (Figure 9f) were found. CD206-as well as CD86-positive cells were also observed around the mineralization area (Figure 8o, l).

The tissue volumes of EDC-nHAC/CaP 40, AA/CC-nHAC/CaP 40, and Terdermis®/CaP 40 at 28 days after implantation, as measured by micro-CT, were 6.4 ± 2.9, 0.9 ± 0.1, and 4.5 ± 2.5 mm^3, respectively. The tissue volume of AA/CC-nHAC/CaP 40 was significantly smaller than that of EDC-nHAC/CaP 40 or Terdermis®/CaP 40, whereas there was no significant difference between the tissue volumes of EDC-nHAC/CaP 40 and Terdermis®/CaP 40. Table 2 shows the newly formed mineralization area and the remaining scaffold area, as measured by histological analysis at 28 days. The remaining scaffold area did not significantly differ between nHAC/CaP 40 samples, and ectopic bone or mineralization was not distinctly observed in HAC/CaP 40 samples. In comparison, ectopic mineralization was observed in only the Terdermis®/CaP 40 sample upon histological observation. Micro-CT analysis also supported this result (Figure 10).

Table 3 shows the ratio of BMP-2 staining cell number/total cell number at 28 days. The ratio of BMP-2 staining cells/total cell number did not significantly differ between nHAC/CaP 10 and CaP 40. The ratio of Terdermis®/CaP 40 was significantly higher than that of Terdermis®/CaP 10, whereas was no significant difference was observed between

scaffold/CaP40 groups. In comparison with that at 4 and 28 days after implantation, the ratio of BMP-2 staining cells/total cell number did not significantly differ between Terdermis®/CaP 10 and CaP 40.

4. Discussion

In the present *in vivo* study, we investigated the yield, releasing period, and activity of BMP-2 released from cells transfected with DNA-functionalized CaP loaded on various scaffolds. BMP-2 is well known to strongly induce bone formation as well as the differentiation and proliferation of osteoblasts [2, 3]. Because the BMP-2 protein is generally released from natural bone tissue, the prepared scaffolds were implanted in the subcutaneous tissue of the back of rats in this study so that only BMP-2 released from the scaffold could be detected, thus eliminating the influence of endogenous BMP-2 secreted from the host bone. In addition, to provide a dose-equivalent control for the released BMP-2 yield from CaP-loaded scaffolds, we utilized scaffolds that had been incubated with BMP-2 solution (3 ng·mL^{-1}), representing the amount of BMP-2 released by transfected cells as determined in a previous *in vitro* study [30].

The peaks of released BMP-2 concentration from EDC-nHAC/solution and AA/CC-HAC/solution scaffolds were observed at 7 or 4 days, respectively. During the 7-day period, AA/CC- and EDC-nHAC scaffolds were rapidly degraded by up to 50%, following which the degradation rate decreased. This suggests that BMP-2 is released along with nHAC scaffold degradation following scaffold preparation by immersion in BMP-2 solution. This result is in accordance with those of other studies [11,12], which demonstrated that the retained yield of exogenous growth factor was dependent on the biodegradable property of the scaffold. In comparison, the peaks of the released BMP-2 concentrations in the Terdermis®/solution groups were observed during the period from 4 to 14 days, although according to histological observation, the collagen scaffold was retained until 28 days following implantation. As SEM

observation demonstrated high porosity of Terdermis®, the BMP-2 protein absorbed on Terdermis® might therefore have been easily released in an early stage.

When combined with CaP, the largest yield of released BMP-2 in the EDC-nHAC/CaP, AA/CC-nHAC/CaP, and Terdermis®/CaP groups was 8.3, 7.3 and 6.1ng·mL^{-1} at 28, 28 and 7 days, respectively. These values were higher than those reported in a previous report (0.2–2.0 ng/implant BMP-2) [21], suggesting that the efficiency of gene transfection by nHAC/CaP was better than that of the previously utilized vector. The larger yield of BMP-2 obtained in the present study might also be attributable to the low cytotoxicity of the scaffold (nHAC) and the CaP vector. In particular, the released BMP-2 yields of all the scaffold groups including Cap were significantly higher than that of the scaffold including naked plasmid DNA. The effective protection of exogenous plasmid DNA from degradation by DNase or inflammatory reactions [27] provided by the multi-CaP shell might also have contributed to the increased yield. Notably, the released BMP-2 concentration in both the EDC- and AA/CC-nHAC/CaP groups increased with the progression of scaffold degradation and the yield of released BMP-2 was significantly higher than those of the nHAC only and nHAC/solution groups.

To evaluate the effect of gradual BMP-2 release from the scaffolds in present study, we analysed ALP as a marker for the early stage of bone formation [12]. The ALP activity in the nHAC/CaP groups and Terdermis®/CaP40 was significantly higher than that of the scaffold only and scaffold/solution groups at 21 and 28 days. Specifically, the increase of ALP activity suggested the occurrence of a biochemical step of bone formation. Thus, the result indicated that the BMP-2 released following gene transfection exhibited a biochemical activity and stimulated the cells surrounding nHAC to differentiate into osteoblasts.

According to histological analysis, the mononuclear cells or multi-nuclear giant cells attached to the degraded nHAC fragments, mineralization area, or collagen. The mononuclear cells were stained with CD 86 or CD 206, which indicates that these cells were consistent with macrophages, whereas the multi-nuclear giant cells were histopathologically consistent

with foreign body giant cells. Furthermore, some of these cells were stained with an anti-BMP-2 antibody. These results indicated that the CaP vector was successfully transfected into the macrophages or foreign body giant cells upon scaffold degradation and that these cells subsequently translated and released BMP-2. Alternatively, in the Terdermis®/CaP group, macrophages or fibroblasts were stained with an anti-BMP-2 antibody during immunohistochemical assessment, indicating that fibroblasts or macrophages infiltrated into Terdermis® took up CaP nanoparticles, resulting in gene transfection followed by BMP-2 expression.

In general, two mechanisms are considered to mediate the uptake of CaP vectors or growth factors combined with scaffolds. In the first pathway, the cells invade the scaffold and take up the growth factor vector [32]. In this case, the pore size is associated with the success of gene transfection of the surrounding cells but not with the degradation speed of the main scaffold. In the second pathway, the growth factors or vectors are released with the degradation of the scaffold allowing the cells surrounding the degraded scaffold to take up the growth factor vector [33, 34]. In this case, the degradation speed of the main scaffold affects the efficacy of gene transfection of the surrounding cells. Therefore, the former mechanism of CaP and growth factor uptake may be utilized for the Terdermis® scaffold whereas the nHAC scaffolds may incorporate both mechanisms based on the results obtained in this study. However, the detail mechanism(s) of the transfection pathway into cells was not clear in this study. We previously demonstrated that the gene transfection pathway or efficiency was dependent on cell type or vector concentration [35].

Macrophages have several phenotypes, with type 1 macrophages (M1) being stained with CD 86 and type 2 macrophages (M2) with CD 206. M1 is associated with inflammation and the secretion of pro-inflammatory cytokines, whereas M2 is associated with matrix deposition, tissue remodelling, healing promotion, and the secretion of pro-regenerative cytokines [36]. In the present study, a larger quantity of M1 than M2 macrophages was observed around the

degraded nHAC fragments or collagen in all scaffold/CaP 40 samples. This suggests that the implanted area may be in a regeneration stage. Consistent with this, new mineralization was formed in the Terdermis®/CaP 40 sample at 28 days after implantation. However, no ectopic mineralization was observed in the other Terdermis®/CaP, Terdermis®/solution, or Terdermis®/plasmid samples in the present study. The suitability of collagen as a scaffold for BMP-2 to facilitate ectopic bone formation has been demonstrated by numerous studies [2,4,12,13,34]. However, whereas constant higher concentration of BMP-2 release might induce ectopic mineralization, low concentration of released BMP-2 might not be sufficient to support ectopic hard tissue formation.

In nHAC/CaP 40 groups, ectopic bone or mineralization was not obviously observed upon H-E and Masson Trichrome staining in either group. However, TRAP- as well as OCN-positive cells were observed in both groups, suggesting the occurrence of hard tissue formation in these groups. In comparison, Oda et al. reported the generation of ectopic bone-like tissue by hydroxyapatite fibre combined with naked pEGFPN1 plasmid (10 μg) encoding BMP-2 in rat beginning at 12 weeks [37], which suggests that ectopic bone formation might be clearly observed in the current study over a longer time period. Furthermore, the volume of hard tissue calculated based on micro-CT 3D image for EDC-nHAC/CaP 40 was significantly larger than that for AA/CC-nHAC/CaP 40. Notably, cross-linking agents have been reported to influence cellular activity, such as adhesion, apoptosis, and proliferation [38, 39]. Consistent with this, more M1 macrophages surrounded fragments in AA/CC-nHAC/CaP40 than EDC-nHAC/CaP samples based on immunohistochemical observation, which might result in smaller hard tissue volume on micro-CT 3D imaging of the respective samples. Moreover, as Wilson et al reported that copper ions hinder bone resorption [40], it is also possible that the different cross-linking agent might have induced different metabolism with regard to hard tissue formation.

In the scaffold with CaP having a higher concentration of CaP nanoparticles (40 μL), however, the yield of released BMP-2 was approximately 6.0–8.0 $ng \cdot mL^{-1}$ at any time point. The slope in the relationship between released BMP-2 and scaffold in the scaffold/CaP 40 groups was 0.02 or −0.02, which indicated that high yields of BMP-2 were constantly released independent of the degradation of nHAC scaffolds, although the slope in the scaffold with CaP (under 20 μL) was −0.1. These results suggested that the maximum limit of BMP-2 release by local gene transfection might be reached *in vivo*, although the released BMP-2 yield by the CaP gene transfection vector was in inverse proportion to scaffold degradation in CaP (under 20 μL). CaP vectors in the scaffold were taken up by the gathered cells such as macrophages or foreign body giant cells in time-dependent manner, whereas in 40 μL CaP with 9.8 μL plasmid DNA, more CaP nanoparticles could be taken up by the gathered cells from in an early stage and sufficient volume of CaP nanoparticles could be retained in the stage of tissue regeneration, resulting in constant BMP-2 release. The number of gathered cells in a local area might be associated with maximum BMP-2 releasing yield. The ratio of BMP-2 staining cells/total cell number did not significantly differ between all scaffold/CaP 40 samples in the present study.

5. Conclusions

In the present study, we determined the degree of BMP-2 release from the scaffolds in rat subcutaneous tissue after the implantation of scaffolds. We demonstrated successful gene transfection *in vivo* using DNA-functionalized CaP combined with nHAC or Terdermis®. We revealed that BMP-2, which resulted from gene transfection mediated by the CaP loaded on the scaffolds, was effectively released into the implanted area and that the released yield of BMP-2 was dependent on the loading CaP concentration. The BMP-2 releasing period of scaffolds with CaP was longer than that of scaffolds that had been immersed in BMP-2 solution or naked plasmid for all scaffolds. In particular, histological evidence demonstrated

that DNA-functionalized CaP combined with Terdermis® formed ectopic mineralization and that DNA-functionalized CaP combined with both nHAC led to the occurrence of ectopic hard tissue formation in subcutaneous tissue at 28 days. In summary, the combination of collagen-based scaffolds and multi-shell CaP nanoparticles loaded with exogenous DNA is expected to comprise a novel gene therapy strategy for tissue regeneration.

Acknowledgements

The authors would like to give our thanks to Prof. Yoshimi Niwano (Tohoku University Graduate School of Dentistry) for his valuable advice regarding the statistical analyses. This work was financially supported by a Grant-in-Aid for Scientific Research (No. 26861667) from the Japan Society for the Promotion of Science.

Conflict of Interest

The authors declare no conflicts of interest associated with this manuscript.

References

[1] R. Rai, R. Raval, R.V. Khandeparker, S.K. Chidrawar, A.A. Khan, M.S. Ganpat, Tissue engineering: step ahead in maxillofacial reconstruction, J Int Oral Health 7 (2015) 138–142.

[2] C. Chu, J. Deng, L. Liu, Y. Cao, X. Wei, J. Li, Y. Man, Nanoparticles Combined with Growth Factors: Recent Progress and Applications, RSC Advances. 6 (2016) 90856-90872.

[3] D. Gothard, E.L. Smith,, J.M. Kanczler, H. Rashidi, O. Qutachi, J. Henstock, M. Rotherham, A. El. Haj, K.M. Shakesheff, R.O. Oreffo, Tissue engineered bone using select growth factors: A comprehensive review of animal studies and clinical translation studies in man, Eur Cell Mater. 28 (2014) 166–207.

[4] M.R.de. Misquita, R. Bentini, F. Goncalves, The performance of bone tissue engineering scaffolds in in vivo animal models: A systematic review, J Biomater Appl. 31 (2016) 625–636.

[5] T. Tenkumo, T. Sugaya, M. Kawanami, F. Watari, Effects of nano-hydroxyapatite content on bone formation in nano-hydroxyapatite-collagen composite membrane with BMP-2 application, Nano Biomedicine. 1 (2009) 159–166.

[6] R. Ishizuka, H. Miyaji, T. Sugaya, M. Kawanami, Periodontal regeneration by BMP-2 solution and collagen hydrogel application to root dentin surface, J. Jap. Soc. Periodontol. 48 (2006) 255–266.

[7] P.M. Bartold, C.A. McCulloch, A.S. Narayanan, S. Pitaru, Tissue engineering: a new paradigm for periodontal regeneration based on molecular and cell biology, Periodontol 2000. 24 (2000) 253–269.

[8] A.M. Makhdom, R.C. Hamdy, The role of growth factors on acceleration of bone regeneration during distraction osteogenesis, Tissue Eng. Part. B. Rev. 19 (2013) 442–453.

[9] H. Tamagawa, T. Tenkumo, T. Sugaya, M. Kawanami. Effect of nanohydroxyapatite on bone morphogenetic protein-2-induced hard tissue formation and dentin resorption on a dentin surface, Appl Surf Sci. 262 (2012) 140–145.

[10] K.D. Hankenson, K. Gagne, M. Shaughnessy, Extracellular signaling molecules to promote fracture healing and bone regeneration, Adv Drug Deliv Rev. 94 (2015) 3–12.

[11] N. Saito, T. Okada, H. Horiuchi, H. Ota, J. Takahashi, N. Murakami, M. Nawata, S. Kojima, K. Nozaki, K. Takaoka, Local bone formation by injection of recombinant human bone morphogenetic protein-2 contained in polymer carriers, Bone. 32 (2003) 381–386.

[12] M. Yamamoto, Y. Takahashi, Y. Tabata, Controlled release by biodegradable hydrogels enhances the ectopic bone formation of bone morphogenetic protein, Biomaterials. 24 (2003) 4375–4383.

[13] A. Kanematsu, S. Yamamoto, M. Ozeki, T. Noguchi, I. Kanatani, O. Ogawa, Y. Tabata, Collagenous matrices as release carriers of exogenous growth factors, Biomaterials. 25 (2004) 4513–4520.

[14] J.N. Zara, R.K. Siu, X. Zhang, J. Shen, R. Ngo, M. Lee, W. Li, M. Chiang, J. Chung J. Kwak, B.M. Wu, K. Ting, C. Soo, High doses of bone morphogenetic protein 2 induce structurally abnormal bone and inflammation in vivo, Tissue Eng Part A. 17 (2011) 1389–1399.

[15] T. Tenkumo, H. Miyaji, T. Sugaya, M. Kawanami, Effect of different dentin conditionings on hard tissue formation and dentin resorption by rhBMP-2 application to the dentin surface, J. Jap. Soc. Periodontol. 47 (2005) 269–279.

[16] J. Jiang, C.Y. Fan, B.F. Zeng, Experimental construction of BMP2 and VEGF gene modified tissue engineering bone in vitro, Int J Mol Sci. 12 (2011) 1744–1755.

[17] Y. Zhang, W. Fan, L. Nothdurft, C. Wu, Y. Zhou, R. Crawford, Y. Xiao, In vitro and in vivo evaluation of adenovirus combined silk fibroin scaffolds for BMP-7 gene delivery, Tissue Eng Part C Methods. 17 (2011) 789–797.

[18] R.G. Crystal, Transfer of genes to humans: early lessons and obstacles to success, Science. 270 (1995) 404–410.

[19] C. Qiao, K. Zhang, H. Jin, L. Miao, C. Shi, X. Liu, A. Yuan, J. Liu, D. Li, C. Zheng, G. Zhang, X. Li, B. Yang, H. Sun, Using poly(lactic-co-glycolic acid) microspheres to encapsulate plasmid of bone morphogenetic protein 2/polyethylenimine nanoparticles to promote bone formation in vitro and in vivo, Int J Nanomedicine. 8 (2013) 2985–2995.

[20] K. Kizjakina, J.M. Bryson, G. Grandinetti, T.M. Reineke, Cationic glycopolymers for the delivery of pDNA to human dermal fibroblasts and rat mesenchymal stem cells, Biomaterials. 33 (2012) 1851–1862.

[21] L.C. Rose, C. Kucharski, H.Uludağ, Protein expression following non-viral delivery of plasmid DNA coding for basic FGF and BMP-2 in a rat ectopic model, Biomaterials. 33 (2012) 3363–3374.

[22] M. Baake, D. Doenecke, W. Albig, Characterisation of nuclear localisation signals of the four human core histones, J Cell Biochem. 81 (2001) 333–346.

[23] D. Delgado, A. del Pozo-Rodríguez, M.Á. Solinís, A. Rodríguez-Gascón, Understanding the mechanism of protamine in solid lipid nanoparticle-based lipofection: the importance of the entry pathway, Eur J Pharm Biopharm. 79 (2011) 495–502.

[24] Y.J. Park, J.F. Liang, K.S. Ko, S.W. Kim, V.C. Yang, Low molecular weight protamine as an efficient and nontoxic gene carrier: in vitro study, J Gene Med. 5 (2003) 700–711.

[25] V. Sokolova, O. Prymak, W. Meyer-Zaika, H. Cölfen, H. Rehage, A. Shukla, M. Epple, Synthesis and characterisation of DNA-functionalised calcium phosphate nanoparticles, Materialwiss Werkst. 37 (2006) 441–445.

[26] M. Epple, A. Kovtun, Functionalized calcium phosphate nanoparticles for biomedical application, Key Eng Mat. 441 (2010) 299–305.

[27] M. Epple, K. Ganesan, R. Heumann, J. Klesing, A. Kovtun, S. Neumann, V. Sokolova, Application of calcium phosphate nanoparticles in biomedicine, J Mater Chem. 20 (2010) 18–23.

[28] S. Chernousova, J. Klesing, N. Soklakova, M. Epple, A genetically active nano-calcium phosphate paste for bone substitution, encoding the formation of BMP-7 and VEGF-A, RSC Adv. 3 (2013) 11155–11161.

[29] V.V. Sokolova, I. Radtke, R. Heumann, M. Epple, Effective transfection of cells with multi-shell calcium phosphate-DNA nanoparticles, Biomaterials 27 (2006) 3147–3153.

[30] T. Tenkumo, J.R. Vanegas Sáenz, Y. Takada, M. Takahashi, O. Rotan, V. Sokolova, M. Epple, K. Sasaki, Gene transfection of human mesenchymal stem cells with a nano-hydroxyapatite-collagen scaffold containing DNA-functionalized calcium phosphate nanoparticles, Genes Cells. 21 (2016) 682–695.

[31] G. Bhakta, S. Mitra, A. Maitra, DNA encapsulated magnesium and manganous phosphate nanoparticles: potential non-viral vectors for gene delivery. Biomaterials. 26 (2005) 2157-2163.

[32] Y. Kuboki, Q. Jin, H. Takita, Geometry of carriers controlling phenotypic expression in BMP-induced osteogenesis and chondrogenesis, J Bone Joint Surg Am. 83 (2001) S105–115.

[33] S. Srouji, D. Ben-David, R. Lotan, E. Livne, R. Avrahami, E. Zussman, Slow-release human recombinant bone morphogenetic protein-2 embedded within electrospun

scaffolds for regeneration of bone defect: in vitro and in vivo evaluation, Tissue Eng Part A. 17 (2011) 269–277.

[34] S. Takemoto, N. Morimoto, Y. Kimura, T. Taira, T. Kitagawa, K. Tomihata, Y. Tabata, S. Suzuki, Preparation of collagen/gelatin sponge scaffold for sustained release of bFGF, Tissue Eng Part A. 14 (2008) 1629–1638.

[35] Vanegas Sáenz JR, Tenkumo T, Kamano Y, Egusa H, Sasaki K. Amiloride-enhanced gene transfection of octa-arginine functionalized calcium phosphate nanoparticles. PLoS One. 16 (2017) doi: 10.1371/journal.pone.0188347. eCollection 2017.

[36] C. Chu, J. Deng, X. Sun, Y. Qu, Y. Man, Collagen membrane and immune response in guided bone regeneration: Recent progress and perspectives, Tissue Engineering Part B Reviews. 23 (2017) 421-435.

[37] M. Oda, S. Kuroda, H. Kondo, S. Kasugai, Hydroxyapatite fiber material with BMP-2 gene induces ectopic bone formation, J Biomed Mater Res B Appl Biomater. 90 (2009) 101–109.

[38] M. Parvizi, J.A. Plantinga, C.A. van Speuwel-Goossens, E.M. van Dongen, S.G. Kluijtmans, M.C. Harmsen, Development of recombinant collagen-peptide-based vehicles for delivery of adipose-derived stromal cells, J Biomed Mater Res A. 104 (2016) 503–516.

[39] C. Chu, J. Deng, L. Xiang, Y. Wu, X. Wei, Y. Qu, Y. Man, Evaluation of nanosized hydroxyapatite (HA) coated epigallocatechin-3-gallate (EGCG) cross-linked collagen membranes, Materials Science and Engineering: C. 78 (2017) 258-264.

[40] T. Wilson, J.M. Katz, D.H. Gray, Inhibition of active bone-resorption by copper, Calcif Tissue Int. 33 (1981) 35–39.

[41] R. Matsui, K. Osaki, J. Konishi, K. Ikegami, M. Koide, Evaluation of an artificial dermis full-thickness skin defect model in the rat, Biomaterials. 17 (1996) 989–994.

Table 1. Final concentrations of calcium phosphate (CaP), DNA-BMP-2, and BMP-2 protein in the nanoparticle dispersions (μg/scaffold).

Sample	Cross-linking agent	CaP	DNA	BMP-2
nHAC/CaP 40	EDC or AA/CC	40.8	9.8	0
nHAC/CaP 20		19.08	4.18	0
nHAC/CaP 10		9.54	2.09	0
nHAC/CaP 4		3.81	0.84	0
nHAC/CaP 2		1.91	0.42	0
nHAC only		0	0	0
nHAC/ Solution		0	0	0.003
nHAC/Plasmid		0	9.8	0
Terdermis®/CaP 40	Heat treatment for 3 h at 110 °C [a)]	40.8	9.8	0
Terdermis®/CaP 20		19.08	4.18	0
Terdermis®/CaP 10		9.54	2.09	0
Terdermis®/CaP 4		3.81	0.84	0
Terdermis®/CaP 2		1.91	0.42	0
Terdermis® only		0	0	0
Terdermis®/Solution		0	0	0.003
Terdermis®/Plasmid		0	9.8	0

a) As reported by Matui et al. [41].

Table 2. Newly-formed mineralization area and the remaining scaffold area in scaffold/CaP 40 at 28 days after implantation.

	EDC-nHAC/CaP 40	AA/CC-nHAC/CaP 40	Terdermis®
Newly formed mineralization area (mm^2)	0 ± 0	0 ±0	3.4 ± 0.3*
Remaining scaffold area (mm^2)	1.9 ± 1.7	1.4 ± 0.9	1.2 ± 0.1

The newly formed mineralization area and the remaining scaffold area were measured by histological analysis. ∗Significant differences ($P < 0.05$) compared to EDC-nHAC/CaP 40.

Table 3. Ratio of BMP-2 staining cells number/total cell number of scaffold/CaP 40 or 10 at 4 and 28 days after implantation.

Sample	Observation time (days)	BMP-2 staining cells/40,000 μm^2	Total cells/ 40,000 μm^2	BMP-2 staining cells/Total cells
EDC-nHAC/CaP 40	4	175 ± 10	251 ± 20	70 ± 6
	28	167 ± 33	266 ± 36	75 ± 3
EDC-nHAC/CaP 10	28	207 ± 61	297 ± 58	69 ± 10
AA/CC-nHAC/CaP 40	4	211 ± 50	324 ± 74	66 ± 7
	28	157 ± 60	224 ± 43	68 ± 7
AA/CC-nHAC/CaP 10	28	174 ± 12	234 ± 39	75 ± 3
Terdermis®/CaP 40	4	110 ± 33 *	141 ± 41*	75 ± 3 *
	28	121 ± 12 *	180 ± 26 *	68 ± 7 *
Terdermis®/CaP 10	28	10 ± 8	74 ± 26	13 ± 6

*Significant differences ($P < 0.05$) compared to the same scaffold/CaP 10.

Figure captions

Figure 1. Schematic of the growth factor releasing system from the scaffolds. nHAC and CaP were fabricated separately. a) The fabricated DNA releasing scaffold is degraded by surrounding cells or collagenase *in vivo* in a timely manner and CaP nanoparticles are released around the tissue. The nanoparticles are taken up by the surrounding cells that then release special growth factor proteins. **b)** Schematic of the CaP nanoparticle fabrication procedure.

Figure 2. Scanning electron micrographs of the sample microstructures. EDC-nHAC without (a) and d)) and with (g)) CaP nanoparticles. AA/CC-nHAC without (b) and e)) and with (h)) CaP nanoparticles. Terdermis® without (c) and f)) and with (i)) CaP nanoparticles. Original magnifications of a)-c) 250×, d)-i) 4,000 ×. Scale bars = 50 μm and 1 μm, respectively. Both nHAC samples and Terdermis® show porosity with a size of approximately 100–500 μm. Spherical shape-like particles with a size of approximately 200–400 nm are seen to be scattered on the nHAC or Terdermis surface.

Figure 3. Released BMP-2 concentration around the implanted site of EDC-nHAC a), AA/CC-nHAC b), and Terdermis® c) including CaP or BMP-2 solution at 4, 7, 14, 21, and 28 days following implantation. CaP injected into the scaffold at 40 ( ), 20 ( ), 10 ( ), 4 ( ), and 2 μL ( ) concentration; scaffold only ( ) concentration; scaffold including plasmid encoding BMP-2 ( ); scaffold including BMP-2 solution (3 ng·mL^{-1}) ( ). Significant differences ($p < 0.05$) between the groups at each time point are denoted by different superscript letters at the same time point (i.e., bars with the same letter are not

significantly different). d) Comparison of the released BMP-2 concentration from each scaffold/CaP 40. *Significant differences ($p < 0.05$) between the groups at each time point.

Figure 4 *In vivo* time profiles of the remaining ratio of EDC-nHAC (●) and AA/CC-nHAC (▲) following implantation into the back of rats over 28 days a). Correlation diagrams with the percentage of remaining nHAC and the releasing yield of BMP-2 from EDC-nHAC/CaP 40 (●), EDC-nHAC/CaP 10 (▲), or EDC-nHAC/solution (◆) b) and AA/CC-nHAC/CaP 40 (●), AA/CC-nHAC/CaP 10 (▲), or AA/CC-nHAC/solution (◆) c) after implantation into the back.

Figure 5. ALP activity of tissues surrounding the implanted site of nHACs cross-linked with EDC (a), nHACs cross-linked with AACC (b), and Terdermis® (C) including CaP or BMP2 solution at 4, 7, 14, 21, and 28 days after implantation. CaP injected into the scaffold at 40( ), 20 ( ), 10 ( ), 4 ( ), and 2 μL ( ) concentration; scaffold only ( ) concentration; scaffold including plasmid encoding BMP-2( ); scaffold including BMP-2 solution (3 $ng \cdot mL^{-1}$) ( ). Significant differences ($p < 0.05$) between the groups at each time point are denoted by different superscript letters at the same time point (i.e., bars with the same letter are not significantly different).

Figure 6. OCN activity of tissues surrounding the implanted site of each scaffold and tissue only at 28 days after implantation. *Significant differences ($p < 0.05$) between the groups.

Figure 7. Immunohistochemical staining with BMP-2; images of scaffold implantation sites at 4 and 28 days after implantation in the back of rats are shown. The left column shows the histology of EDC-nHAC/CaP 40 at 4 days, stained by haematoxylin and eosin (H-E) (a), and BMP-2 stain (d). EDC-nHAC/CaP 40 at 28 days stained by H-E (g) and BMP-2 stain (j).

EDC-nHAC/CaP 10 at 28 days stained by H-E (m), and BMP-2 stain (p). Centre column shows AACC-nHAC/CaP 40 at 4days stained by H-E (b), and BMP-2 stain (e). AA/CC-nHAC/CaP 40 at 28 days stained by H-E (h) and BMP-2 stain (k). AA/CC-nHAC/CaP 10 at 28 days stained by H-E (n) and BMP-2 stain (q). Right column shows Terdermis®/CaP 40 at 4 days stained by H-E (c), and BMP-2 stain (f). Terdermis®/CaP 40 at 28 days stained by H-E (i), and BMP-2 stain (l). Terdermis®/CaP 10 at 28 days stained by H-E (0), and BMP-2 stain (r). White arrowhead indicates BMP-2-positive area. Asterisks indicate the retained nHAC. Scale bars: 50 μm.

Figure 8. Histologic images of scaffold implantation sites at 28 days after implantation in the back of rats. Histology of EDC-nHAC/CaP 40 (left column; a, d, g), AACC-nHAC/CaP 40 (centre column, b, e, h), and Terdermis®/CaP 40 (right column, c, f, i) stained by haematoxylin and eosin (H-E) with low magnifications (a-c), H-E with high magnification (d-f), Masson Trichrome (g-i), CD 206 (j-l), and CD 86 (m-o). Asterisks indicate the retained scaffold. White arrows indicate newly formed mineralization. Black arrows head indicate CD206-positive cells. White arrows head indicate the CD86-positive cells. Scale bars: 200 μm (a-c) and 50 μm (d-o).

Figure 9. Immunohistochemical image of scaffold implantation sites at 28 days after implantation in the back of rats. The left column shows the Histology of EDC-nHAC/CaP 40 (left column, a, d), AACC-nHAC/CaP 40 (centre column, b, e), and Terdermis®/CaP 40 (right column, c, f) stained by TRAP stain (a-c) and OCN (d-f). TRAP-positive cells (black arrows) can be observed around the degraded scaffolds. White arrows indicate the OCN-positive area. White arrows indicate newly formed mineralization. Asterisks indicate the retained nHAC. Scale bars: 50 μm.

Figure 10. Micro-CT images of EDC-nHAC/CaP40 a), AA/CC-nHAC/CaP40 b), and Terdermis®/CaP40 c) at 28 days after implantation in the back of rats. Scale bars: 2 mm.

Highlight

① DNA-functionalized CaP gene transfection vector combined with nano-hydroxyapatite-collagen or collagen scaffolds induce the successful gene transfection *in vivo*.

② Released yield of BMP-2, which resulted from gene transfection, was dependent on the loading CaP concentration.

③ BMP-2 releasing period of scaffolds with CaP gene transfection vector was longer than that of scaffolds that had been immersed in BMP-2 solution.

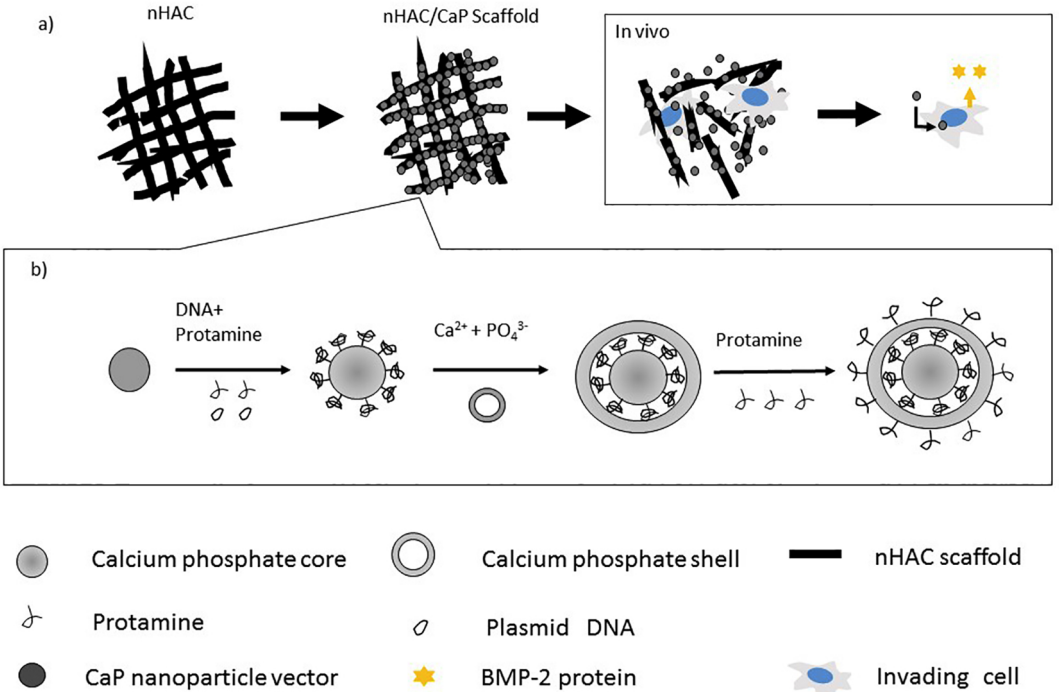
a)
nHAC
nHAC/CaP Scaffold
In vivo
b)
DNA+
Protamine
$Ca^{2+} + PO_4^{3-}$
Protamine
Calcium phosphate core
Calcium phosphate shell
nHAC scaffold
Protamine
Plasmid DNA
CaP nanoparticle vector
BMP-2 protein
Invading cell

Figure 1

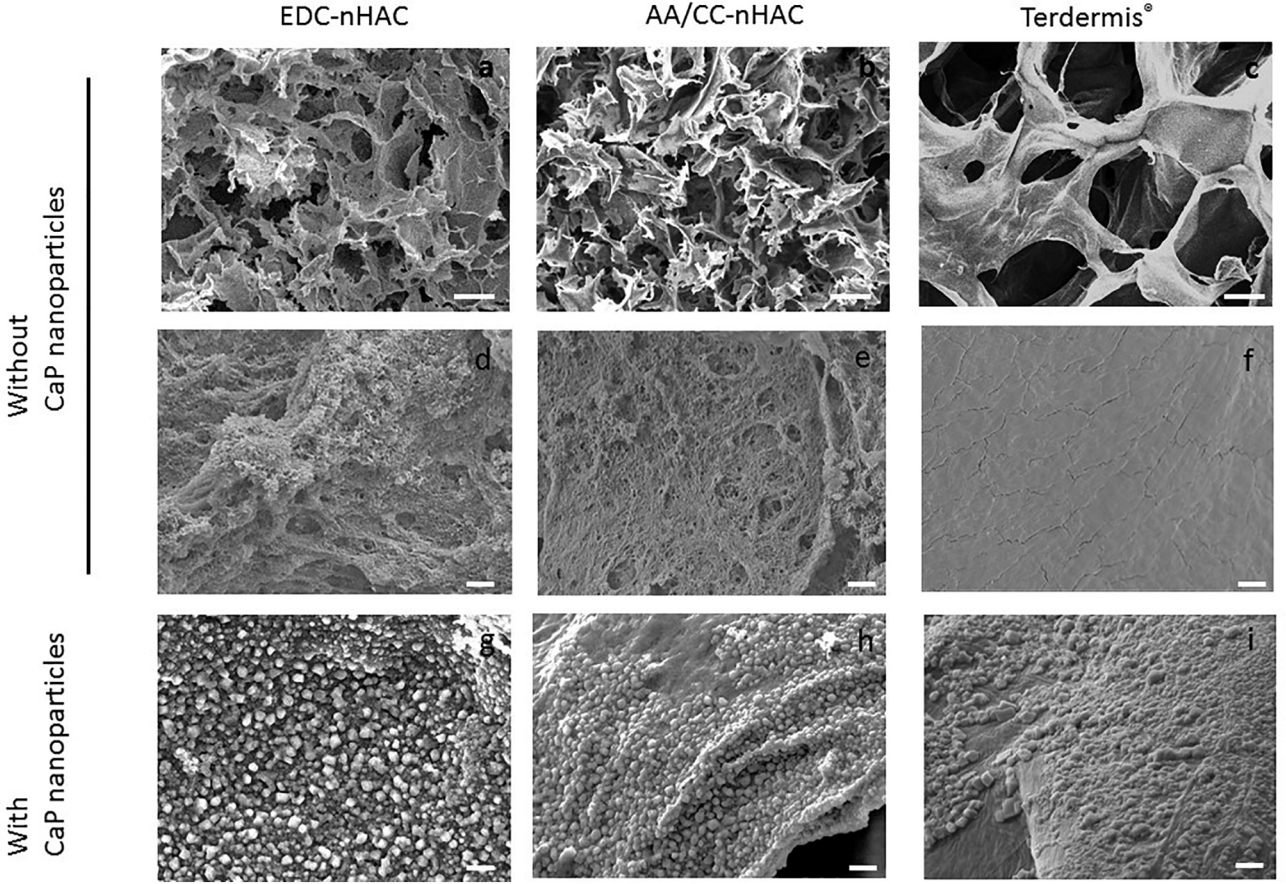
EDC-nHAC
AA/CC-nHAC
Terdermis®
Without CaP nanoparticles
With CaP nanoparticles
a
b
c
d
e
f
g
h
i

Figure 2

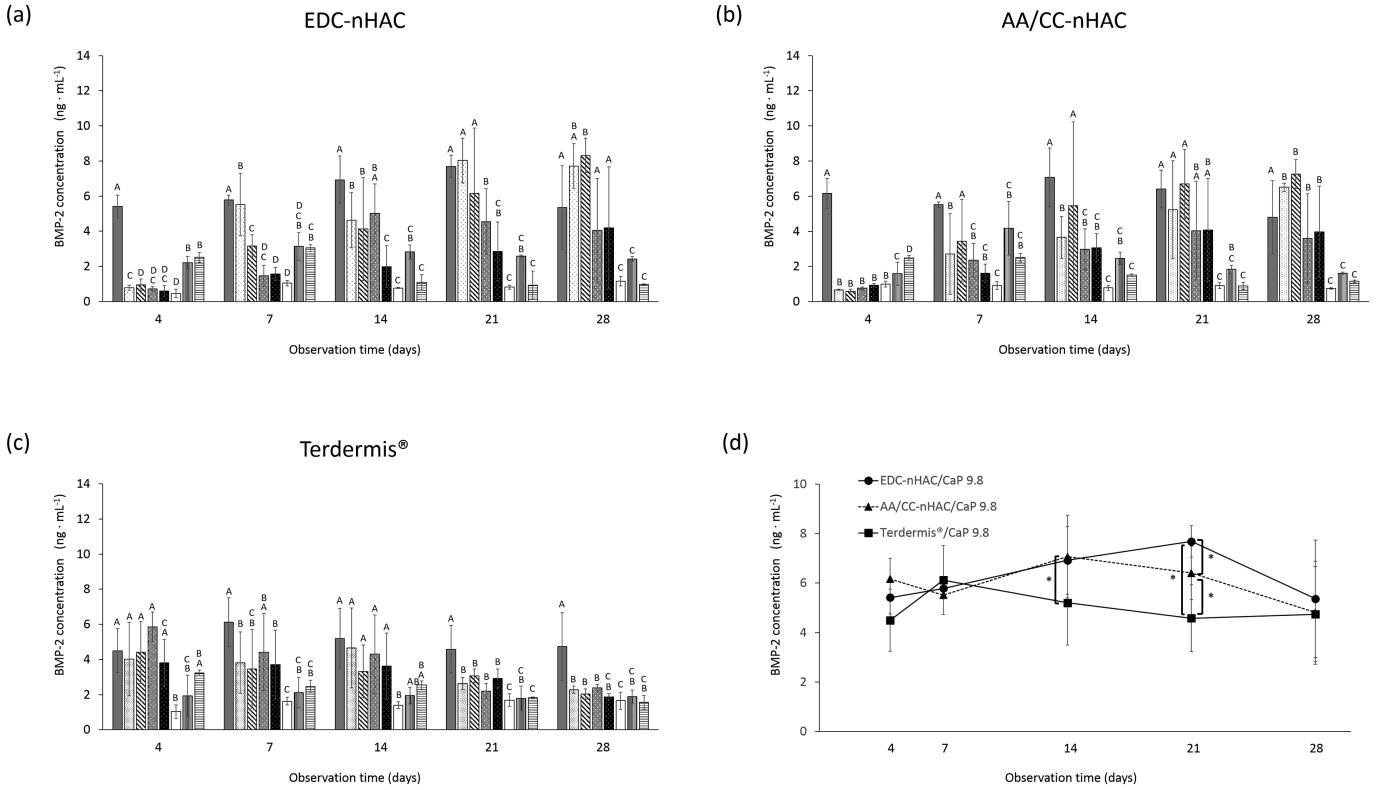
(a)
EDC-nHAC
(b)
AA/CC-nHAC
(c)
Terdermis®
(d)
BMP-2 concentration (ng · mL-1)
Observation time (days)
4
7
14
21
28
EDC-nHAC/CaP 9.8
AA/CC-nHAC/CaP 9.8
Terdermis®/CaP 9.8

Figure 3

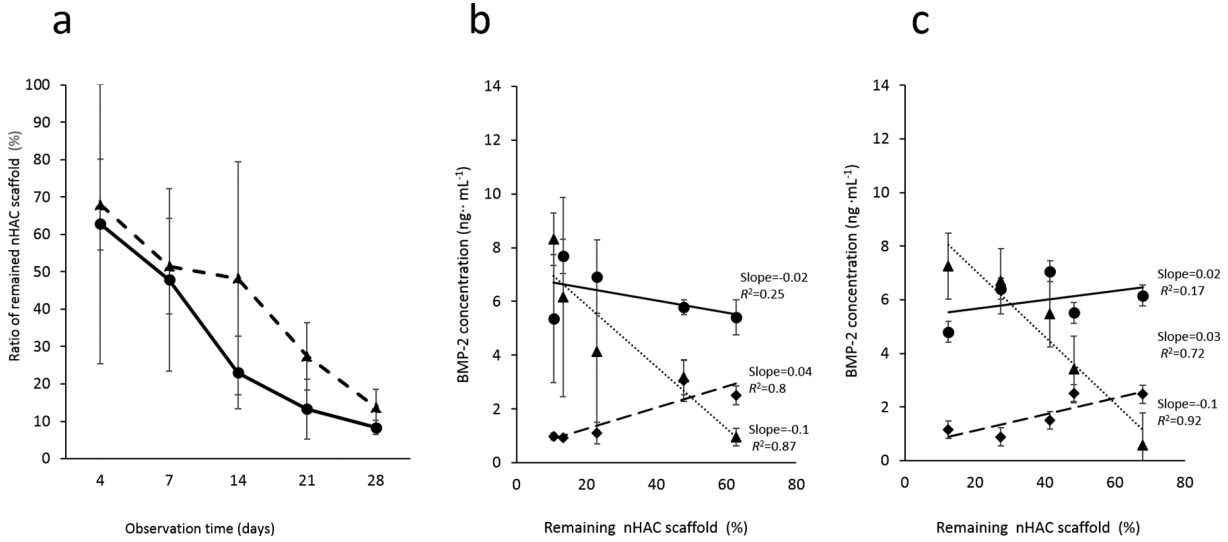
a
b
c
Ratio of remained nHAC scaffold (%)
Observation time (days)
BMP-2 concentration (ng·· mL-1)
Remaining nHAC scaffold (%)
Slope=-0.02
R2=0.25
Slope=0.04
R2=0.8
Slope=-0.1
R2=0.87
BMP-2 concentration (ng ·mL-1)
Slope=0.02
R2=0.17
Slope=0.03
R2=0.72
Slope=-0.1
R2=0.92

Figure 4

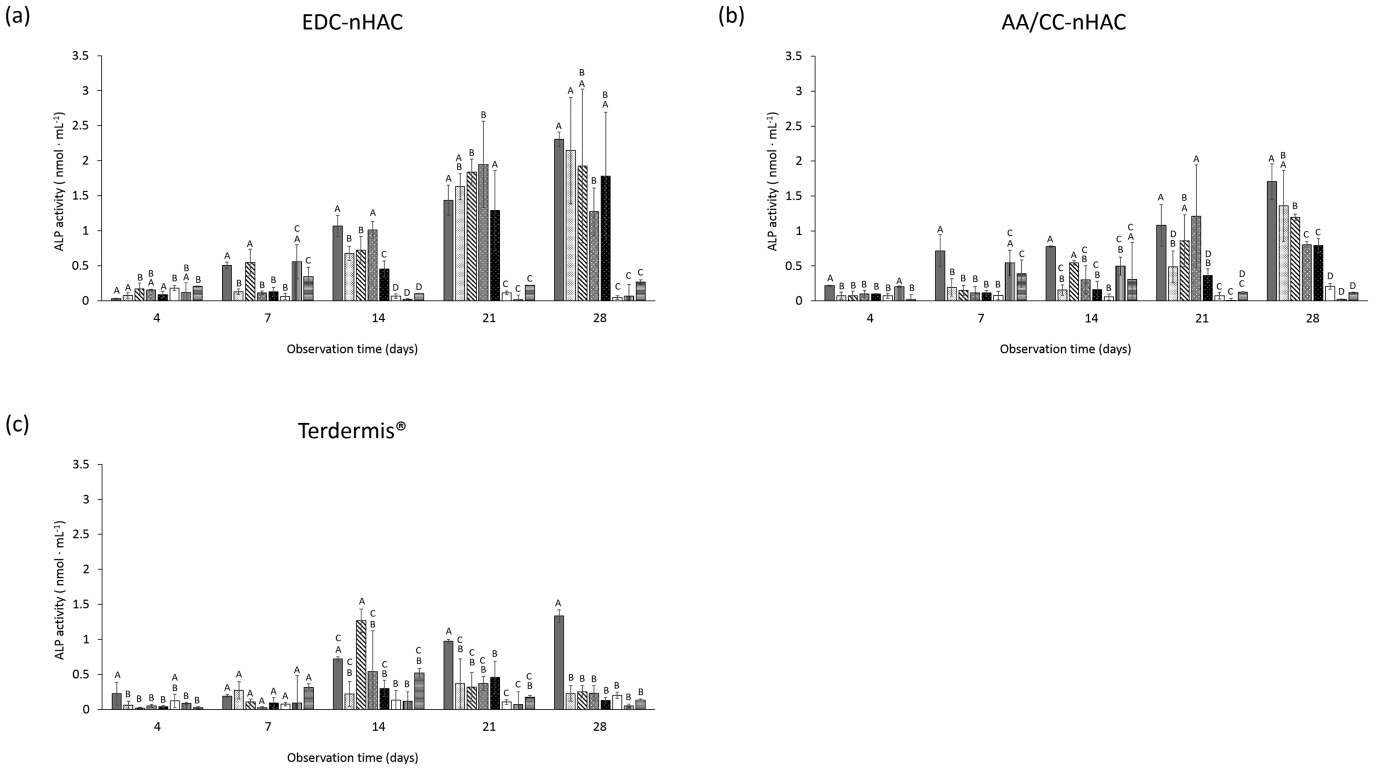
(a)
EDC-nHAC
(b)
AA/CC-nHAC
(c)
Terdermis®
ALP activity (nmol · mL-1)
Observation time (days)
4
7
14
21
28
0
0.5
1
1.5
2
2.5
3
3.5

Figure 5

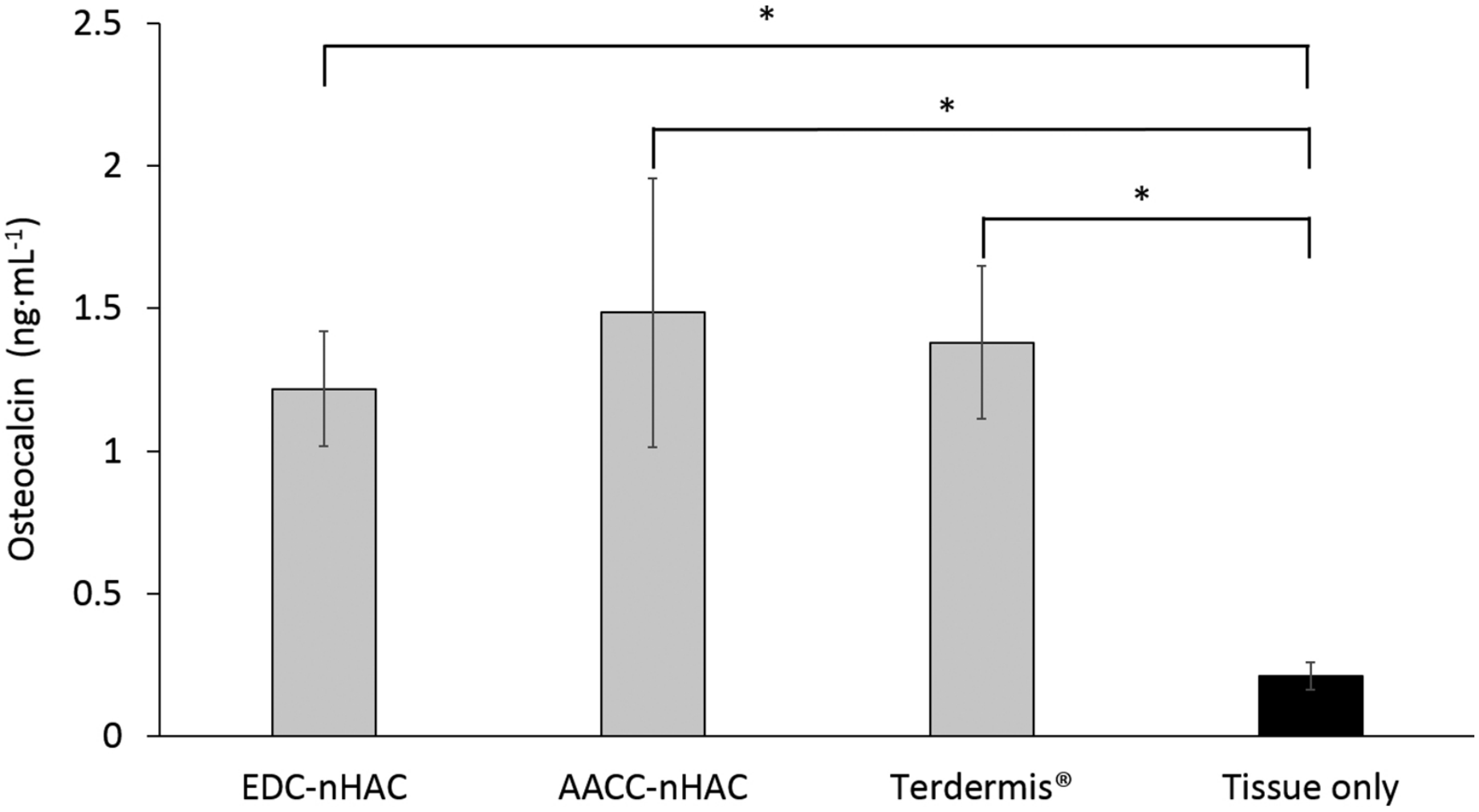
2.5
2
1.5
1
0.5
0
Osteocalcin (ng·mL-1)
*
*
*
EDC-nHAC
AACC-nHAC
Terdermis®
Tissue only

Figure 6

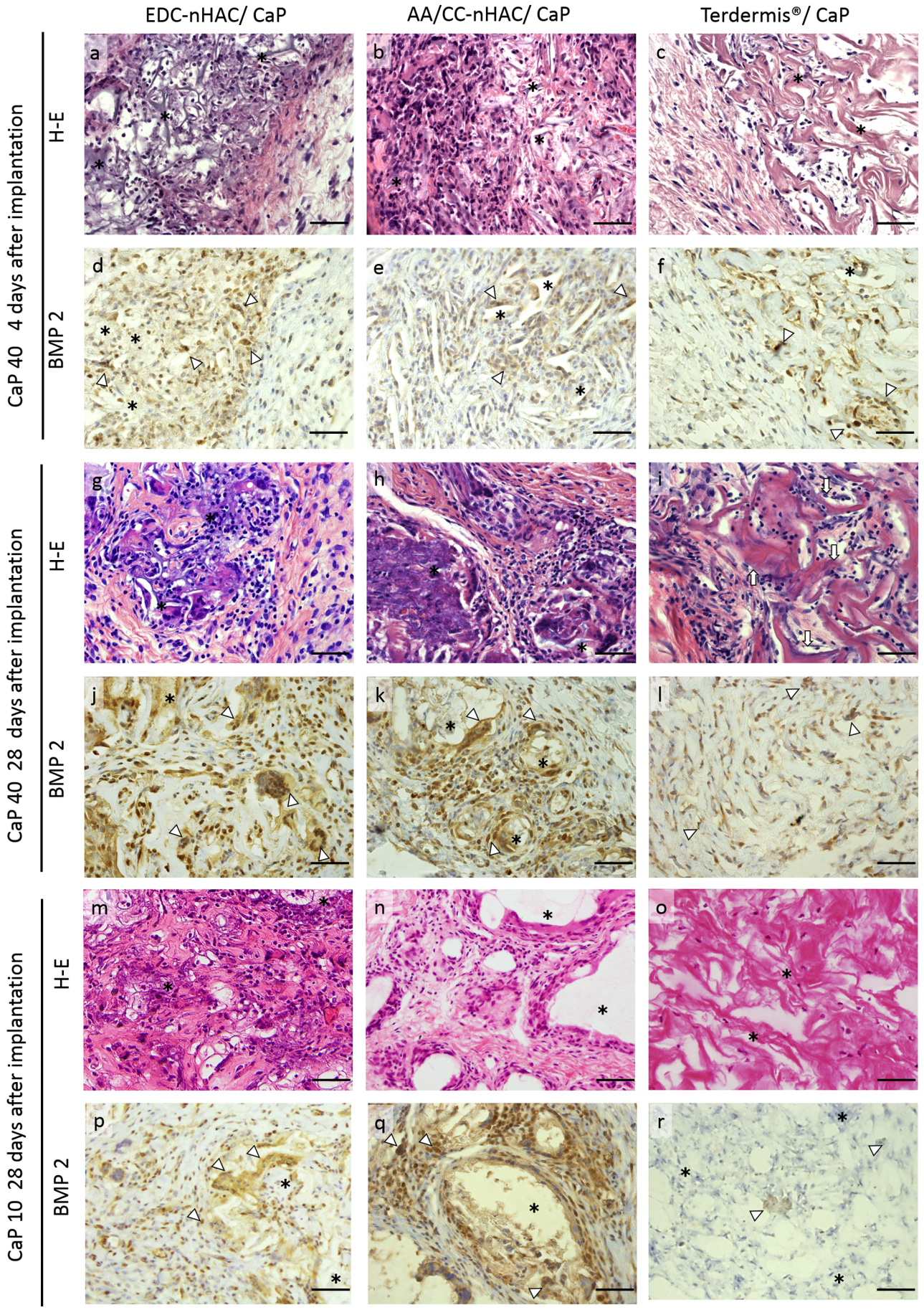
EDC-nHAC/ CaP
AA/CC-nHAC/ CaP
Terdermis®/ CaP
CaP 40 4 days after implantation
CaP 40 28 days after implantation
CaP 10 28 days after implantation
H-E
BMP 2
a
b
c
d
e
f
g
h
i
j
k
l
m
n
o
p
q
r

Figure 7

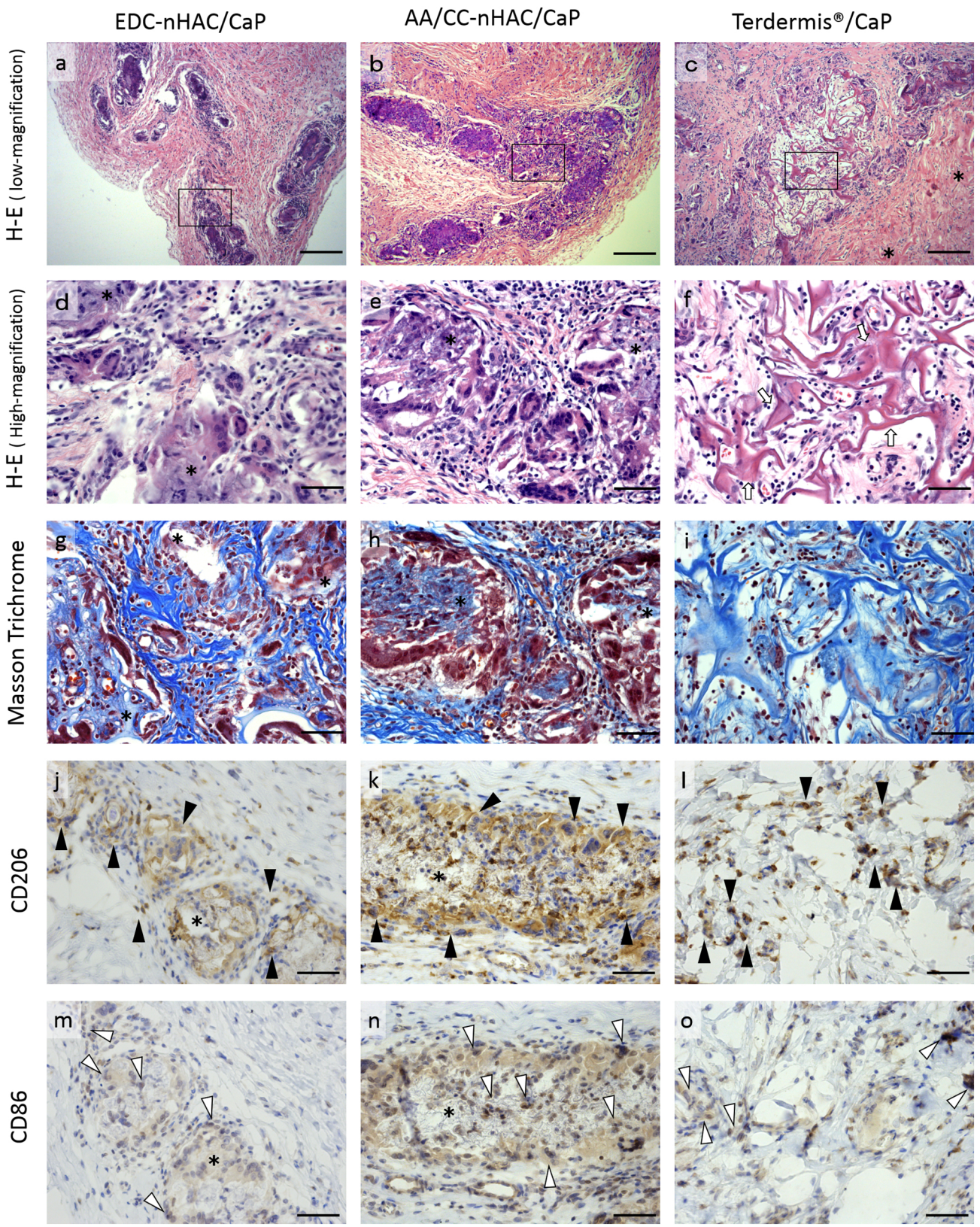
EDC-nHAC/CaP
AA/CC-nHAC/CaP
Terdermis®/CaP
H-E (low-magnification)
H-E (High-magnification)
Masson Trichrome
CD206
CD86
a
b
c
d
e
f
g
h
i
j
k
l
m
n
o

Figure 8

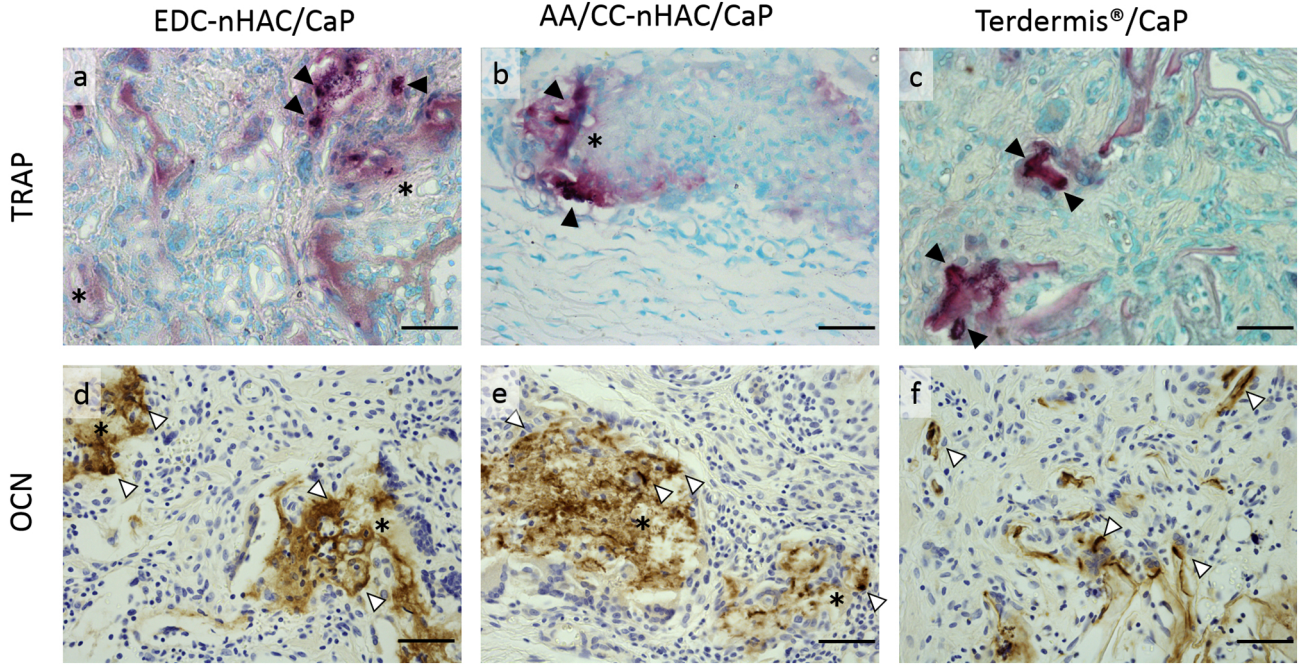

Figure 9

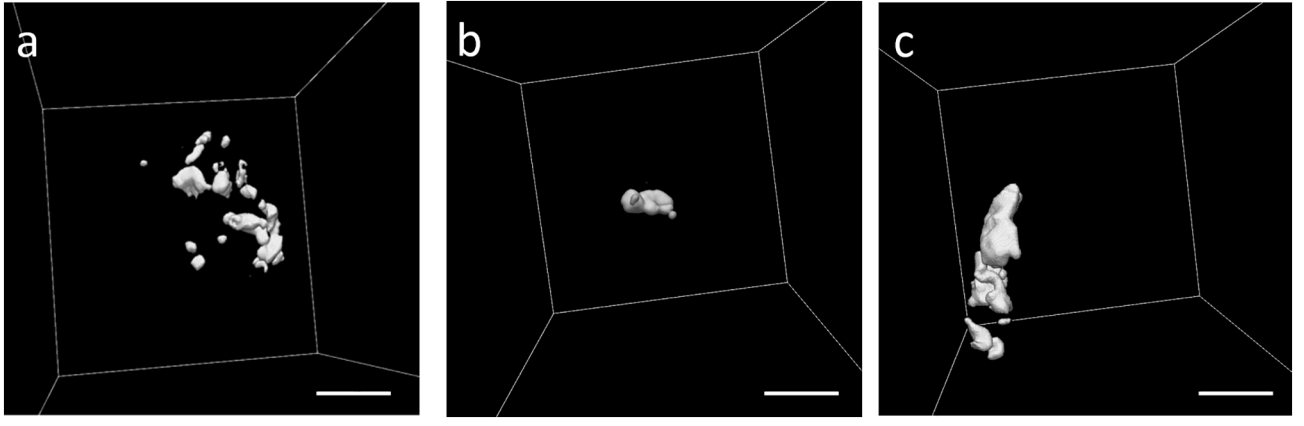

Figure 10